

Sodium binding sites and permeation mechanism in the NaChBac  
channel: a Molecular Dynamics study

Carlo Guardiani

School of Engineering  
University of Warwick, UK

Philip M. Rodger

Department of Chemistry  
University Of Warwick, UK

Olena A. Fedorenko

Division of Biomedical and Life Sciences  
Lancaster University,  
Lancaster, UK

Stephen K. Roberts

Division of Biomedical and Life Sciences  
Lancaster University,  
Lancaster, UK

Igor Khovanov<sup>1</sup>

School of Engineering  
University of Warwick, UK.

<sup>1</sup>Corresponding author. I.Khovanov@warwick.ac.uk

## SUPPORTING INFORMATION

### 1 Supplementary Methods

#### 1.1 Potential of Mean Force

In the unbiased simulation the Potential of Mean Force of sodium ions as a function of the position along the channel axis was computed using an expression proposed by Roux and coworkers (1).

$$\Delta G(z) = -k_B T \log \left( \frac{\rho(z)}{\rho_{bulk}} \right)$$

In 2D-metadynamics the two ions biased to explore the selectivity filter have identical physical properties. This means that it is pointless to discriminate the probabilities  $P(z_1 = a, z_2 = b)$  and  $P(z_1 = b, z_2 = a)$ , because the relevant quantity is the probability that either of the two ions is in  $z = a$  while the remaining ion is in  $z = b$ . The corresponding Potential of Mean Force is

$$\begin{aligned} \Phi(z_1, z_2) &= -k_B T \log \frac{P(z_1, z_2) + P(z_2, z_1)}{2} \\ &= -k_B T \log \frac{e^{-F(z_1, z_2)/k_B T} + e^{-F(z_2, z_1)/k_B T}}{2} \end{aligned}$$

where  $F(z_1, z_2)$  is the PMF yielded from metadynamics and the 1/2 factor in the argument of the logarithm ensures normalization of the  $P(z_1, z_2) + P(z_2, z_1)$  distribution. When the symmetrical  $\Phi(z_1, z_2)$  free energy surface is projected along a single collective variable, it is possible to attain the PMF as a function of the axial distance  $z$  of a biased ion (irrespective of its identity) from the center of mass of the alpha Carbons of the glutamates:  $\Phi(z_1) = \Phi(z_2) = \Phi(z)$  where

$$\Phi(z_1) = -k_B T \log \int e^{-\Phi(z_1, z_2)/k_B T} dz_2$$

$$\Phi(z_2) = -k_B T \log \int e^{-\Phi(z_1, z_2)/k_B T} dz_1$$

#### 1.2 Nudged Elastic Bands

A permeation mechanism can be determined computing on the axial-axial PMF from metadynamics the Minimum Energy Path (MEP) that connects the configurations of the system before and after a permeation event. The calculation

was performed using a modified Nudged Elastic Band method as proposed in Ref (2). The algorithm starts from an initial guess of the MEP represented by a string of points arranged along the straight line connecting the initial and final states. The initial path then converges to the MEP through a simulated annealing Monte Carlo minimization of the energy function

$$E = \sum_{i=1}^{N-1} [k(l_{i,i+1} - l_0) + G(z_i, z'_i)]$$

where  $k = 10 \text{ kcal/mol/\AA}^2$ , and  $l_0 = 0.5 \text{ \AA}$  are tunable parameters representing respectively the force constant of the springs linking the points on the path and the reference distance between neighbouring points. The  $l_{i,i+1}$  is the current value of the distance between points  $i, i + 1$  and  $G(z_i, z'_i)$  represents the free energy on point  $i$ . During annealing the temperature was exponentially decreased from 50 to 1 in 10 million steps.

### 1.3 Markov State Model and Transition Path Theory

The first step in the building of a Markov model is the identification of a set of states involved in

the transitions. Our states are the single, double, triple,  $\dots$ , occupancy states of sites CC, IN, CEN, HFS, S4 and EX. Sites IN, CEN, HFS, S4 are the binding sites in the SF corresponding to the minima of the PMF, while sites CC and EX are two regions respectively below and above the selectivity filter. The next step is to assign the frames of the MD trajectory to the corresponding states and to compute a matrix of transition probabilities. This calculation must be repeated for different lagtimes to determine when the dynamics becomes Markovian. The idea is to start with a lagtime  $\tau = \Delta t$  corresponding to the sampling interval of the MD simulation and to determine the smallest  $n$  such that  $S(n\Delta t) = T(\Delta t)^n$ . When this occurs the plot of implied timescales as a function of the lagtime levels out.

In order to apply Transition Path Theory, the transition probability matrix  $S$  computed during the Markov model building must be used to derive a matrix of the transition rates simply discretizing the Master equation. It will be also necessary to choose a set of initial and final states A, B that in our case represent configurations of the system before and after the per-

meation event respectively. The key quantities involved in TPT are the committor probabilities. The forward committor is the probability that a trajectory leaving state  $i$  reaches  $B$  before reverting to  $A$ . The backward committor on the other hand, is the probability that a trajectory arrived to state  $i$  comes from  $A$  rather than from  $B$ . Based on these definitions and on the theory of Markov chains with absorbing states, it is possible to compute the committor probabilities of all states. It must be considered that the transition rate  $L_{ij}$  includes many non-productive trajectories such as those that never reach the final state  $B$  and those that reach  $B$  without originating from  $A$ . This is why it is convenient to define a probability flux along edge  $(i, j)$  contributing to transition  $A \rightarrow B$ :  $f_{ij} = \pi_i q_i^- L_{ij} q_j^+$ . Since this quantity still includes recrossing events, a net flux along arc  $(i, j)$  will be defined as  $f_{ij}^+ = \max[0, f_{ij} - f_{ji}]$ . Once a net flux has been computed for all arcs of the transition graph, the dominant paths can be identified as those paths with a maximal bottleneck flux, using a variant of Dijkstra's algorithm (3). All calculations were performed with

the MSMBuilder program (4).

## 1.4 Computing Currents through a Collective Diffusion Model

Applying Linear Response Theory Liu and Zhu (5) showed that the steady current induced by a weak constant potential  $V$  can be computed integrating the autocorrelation function of the current at equilibrium, in the absence of any external electric field

$$I_{steady} = \frac{V}{k_B T} \int_0^\infty \langle I(0)I(t) \rangle dt \quad (1)$$

Equation 1 can be simplified considering the net amount of current transported across the channel at equilibrium

$$Q(t) = \int_0^t I(t') dt'$$

It is possible to show that the Mean Square Displacement of  $Q(t)$  is related to the current autocorrelation function by

$$\langle Q^2(t) \rangle = 2 \int_0^t (t - t') \langle I(0)I(t') \rangle dt'$$

Using Einstein relation, the diffusion coefficient of  $Q$  can be computed as

$$D_Q = \frac{1}{2} \lim_{t \rightarrow \infty} \frac{d \langle Q^2(t) \rangle}{dt} = \int_0^\infty \langle I(0)I(t) \rangle dt$$

The current autocorrelation function in Eq 1 can then be substituted by the diffusion coefficient  $D_Q$  yielding

$$I_{steady} = \frac{D_Q}{k_B T} V$$

Accordingly, the channel conductance can be simply computed as

$$\gamma = \frac{I}{V} = \frac{D_Q}{k_B T}$$

### 1.5 Patch-clamp measurements of currents in NaChBac

To date electrophysiological data on NaChBac have been reported using physiological ion concentration (i.e. approximately 150 mM NaCl)

and in contrast, MD simulations are performed in much greater non physiological ion concentrations (for example, 0.5 M NaCl). To address this gap in our understanding we determined NaChBac channel behaviour in symmetrical 0.5 M Na<sup>+</sup> and thus compatible with MD simulations (Figure 11 of main paper and Supp. Figure S7). At these high ion concentrations stability of membranes/recordings was limited to less than 10 minutes; although this limited the scope of recordings, membranes were sufficiently stable to accurately determine single channel current amplitude (Supp. Figure S7 C) and enable accurate calculation of single channel conductance from current voltage plots of NaChBac activity (Figure 11 inset).

NaChBac (GenBank accession number BAB05220) cDNA was synthesised with a C-terminal FLAG epitope by EPOCH Life Science (www.epochlifescience.com), subcloned into the mammalian cell expression vector pTracer-CMV2 (Invitrogen) (at EcoRI and EcoRV sites) and used for transfection of Chinese Hamster Ovary (CHO) cells with TransIT-2020 (Mirus Bio). Transfected cells (expressing GFP)

## NaChBac permeation

---

were identified with an inverted fluorescence microscope (Nikon TE2000-s) and their electrophysiological properties were determined between 24 and 48 hours after transfection.

Patch clamp recordings were acquired using an Axopatch 200A (Molecular Devices, Inc., USA) amplifier and digitized using Digidata1322 (Molecular Devices, Inc., USA) and filtered at 1 kHz. Patch-clamp electrodes were pulled from borosilicate glass (Kimax, Kimble Company, USA) and exhibited resistances of 3-5 M $\Omega$ . The shanks of the pipettes tip were coated with bees wax in order to reduce pipette capacitance. The pipette solution contained (in mM) 492 Na-gluconate, 5 NaCl, 10 EGTA, and 10 HEPES, pH 7.4 (adjusted by NaOH; [Na]<sub>total</sub>=500 mM; 882 mmol/kg). Standard bath solution contained (in mM) 497 NaCl, and 10 HEPES, pH 7.4 (adjusted by NaOH; [Na]<sub>total</sub>=500 mM; 894 mmol/kg). Osmolarities were measured using a Wescor vapor pressure osmometer (model 5520). All solutions were filtered before use. The bath solution in the experimental chamber was continuously exchanged by a gravity-driven flow at rate of approximately 2 ml/min in a chamber

volume of approximately 200  $\mu$ l. The bath solution was grounded using a 3 M KCl agar bridge. The liquid junction potential for solutions, in which G $\Omega$  seals were obtained, was measured to be 5 mV according to the method described by Neher (1992) and was accounted for. Experiments were conducted at room temperature.

To record NaChBac activity in 0.5 M Na<sup>+</sup>, cells were initially bathed in a solution containing relatively low Na<sup>+</sup> content (containing (in mM) 140 NaCl, 10 HEPES and 10 glucose, pH 7.4 (adjusted by NaOH to give a total Na<sup>+</sup> content of 140.5 mM and 244 mmol/kg) for up to 15 minutes to allow for identification of GFP expressing cells and placement of pipette next to a cell. The low Na<sup>+</sup> content bath solution was replaced with one containing (in mM) 248 NaCl, and 10 HEPES, pH 7.4 adjusted with NaOH to give a total Na<sup>+</sup> content of 250 mM and 448 mmol/kg, and G $\Omega$  seals with the pipette were achieved using suction. Immediately after obtaining cell attached configuration, bath solution was exchanged with standard bath solution (containing 0.5 M Na<sup>+</sup>). The flow rate was 2 ml/min which enabled rapid exchange of bath so-

lution and protection from cells bursting as a result of "osmotic shock"; despite this the success rate was less than 10%. Whole cell NaChBac-mediated currents were recorded in response to voltage steps ranging from +65 mV to -55 mV in -20 mV steps from a holding voltage of -95 mV (Figure S7 A). Whole cell peak current-voltage relationship (Figure S7 B) showed that  $E_{rev}$  was approximately at  $E_{Na}$  (0 mV) and did not coincide with  $E_{Cl}$  (-116 mV) consistent with these currents being carried by  $Na^+$ . Immediately after obtaining whole cell configuration either the pipette was pulled away to obtain excised out configuration or whole cell currents were first recorded prior to achieving the outside-out configuration. Channel inactivation typical for that previously reported for NaChBac (6) was observed in high  $Na^+$  content solutions but note that in contrast to reported  $\sim 12$  pS (in 140 mM  $Na^+$ ) the single channel conductance of NaChBac in 0.5 M  $Na^+$  was  $41.4 \pm 0.66$  pS which was similar to that predicted by Linear Response Theory.

## 2 Supplementary Results

### 2.1 Fluctuations in $Na^+$ coordination

The error on hydration and coordination numbers was directly worked out as the standard deviation of the coordination numbers computed in the 5000 frames of the trajectory. The error bars in **Fig-4** of the Main Paper show that the number of coordinating oxygens is subject to significant fluctuations. When sodium visits bin  $[0.0 : 2.0]$  Å (included in the IN binding site that corresponds to the 0-3 Å range), the most frequent arrangements are a 6-water coordination occurring in 68% of cases and a 5-water coordination occurring in a further 24% of cases. In both of these situations sodium does not interact with any protein residue. Interaction with a single protein oxygen (the carbonyl oxygen of a Thr of the SF) occurs only in 1.5% of cases.

The coordination pattern of sodium in site CEN ( $[3 : 7]$  Å range) can be evaluated from an analysis of bin  $[4 : 6]$  Å. Here in 64% of conformations, sodium is coordinated by six water molecules and has no direct interaction with any protein oxygen. In the second most frequent ar-

range, occurring in 16% of cases, sodium interacts with 5 water molecules and a single protein oxygen from the carbonyl group of a Leucine of the SF. As shown in the axial-radial PMF (**Fig-5** of the Main Paper) the loose Na-protein interaction in sites IN and CEN favours an on-axis placement of the sodium ion.

The conformations corresponding to bin [8.0 10.0] Å (included in site HFS that extends over the 7-10 Å range) are extremely heterogeneous since the number of coordinating water oxygens ranges from 2 to 7, the glutamate oxygens from 0 to 2 and the other protein oxygens also from 0 to 2. Many oxygen combinations are thus possible but the most frequent are the one with 4 water oxygens, one glutamate oxygen and another single protein oxygen (29% of cases) and the one with three water oxygens, a glutamate oxygen and another protein oxygen (23% of cases). In both arrangements the second protein oxygen is often contributed by a Serine residue belonging to the same subunit of the coordinating glutamate. As confirmed by the axial-radial PMF of **Fig-5** of the Main Paper, the double interaction of Na<sup>+</sup> with two residues of the SF favours an

off-axis placement.

Finally, in the [10-12] Å range, corresponding to site S4, sodium has 23% and 49% probability to interact with one or two serines respectively. In the 1-serine scenario Na<sup>+</sup> is surrounded by 5 water molecules whereas only 4 will solvate it in the 2-serine arrangement so as to reach the optimal 6-oxygen coordination pattern. In the 2-serine arrangement the two serines belong to the same subunit in about 70% of cases forcing sodium in an off-axial position. These conformations populate the third minimum of the axial-radial PMF of **Fig-5** of the Main Paper.

## References

- [1] Im, W.; Roux, B. Ion permeation and selectivity of OmpF porin: a theoretical study based on molecular dynamics, Brownian dynamics, and continuum electrodiffusion theory. *J. Mol. Biol.* **2002**, 322, 851-869.
- [2] Stock, L.; Delemotte, L.; Carnevale, V.; Treptow, W.; Klein, M.L. Conduction in a Biological Sodium selective Channel. *J. Phys. Chem. B* **2013**, 117, 3782-3789.

- [3] Gupta, A.; Zangrilli, M.; Sundararaj, A.; Dinda, P.A.; Lowekamp, B.B. (2005) Free Network Measurement for Adaptive Virtualized Distributed Computing. *Technical Report NWU-CS-05-13, June 28, 2005* Northwestern University, USA.
- [4] Beauchamp, K.A.; Bowman, G.R.; Lane, T.J.; Maibaum, L.; Haque, I.S.; Pande, V.S. MSMBuild2: Modeling Conformational Dynamics on the Picosecond to Millisecond Scale. *J. Chem. Theory Comput.* **2004**, 7, 3412-3419.
- [5] Liu, Y.; Zhu, F. Collective Diffusion Model for Ion Conduction through Microscopic Channels. *Biophys. J.* **2013**, 104, 368-376.
- [6] Ren, D.; Navarro, B.; Xu, H.; Yue, L.; Shi, Q.; Clapham, D.E. A Prokaryotic Voltage-Gated Channel. *Science* **2001**, 294, 2372-2375.

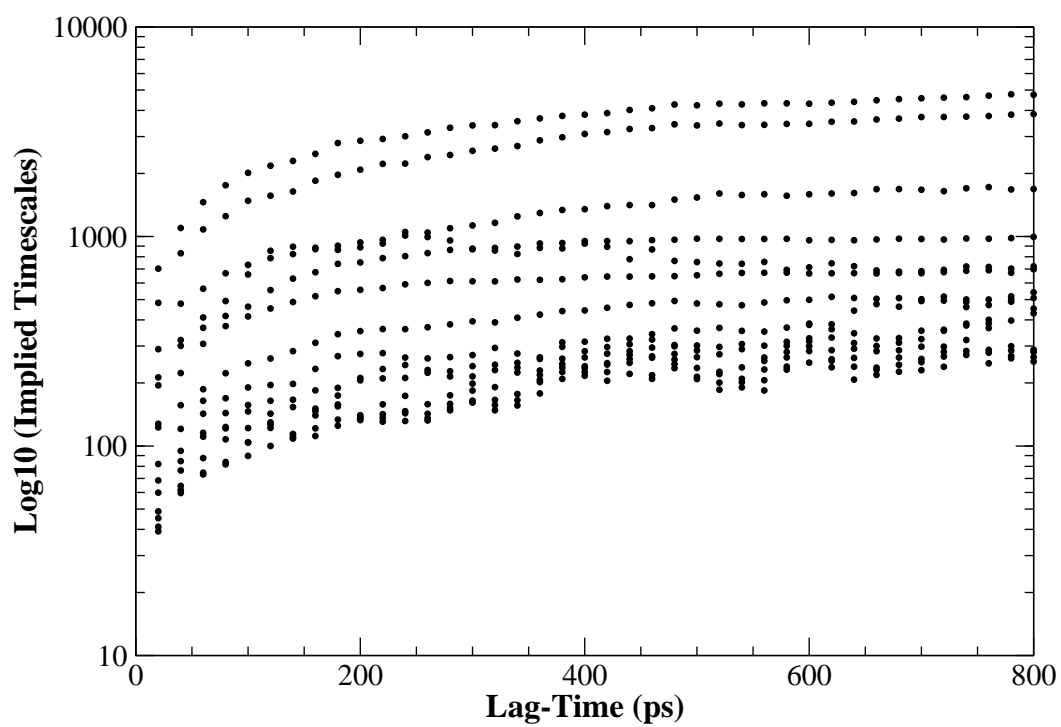


Figure 1: Time scales as a function of lag-time for the Markov State Model of permeation dynamics. At  $\tau=200$  ps the time-scales level out and the dynamics can be regarded as Markovian.

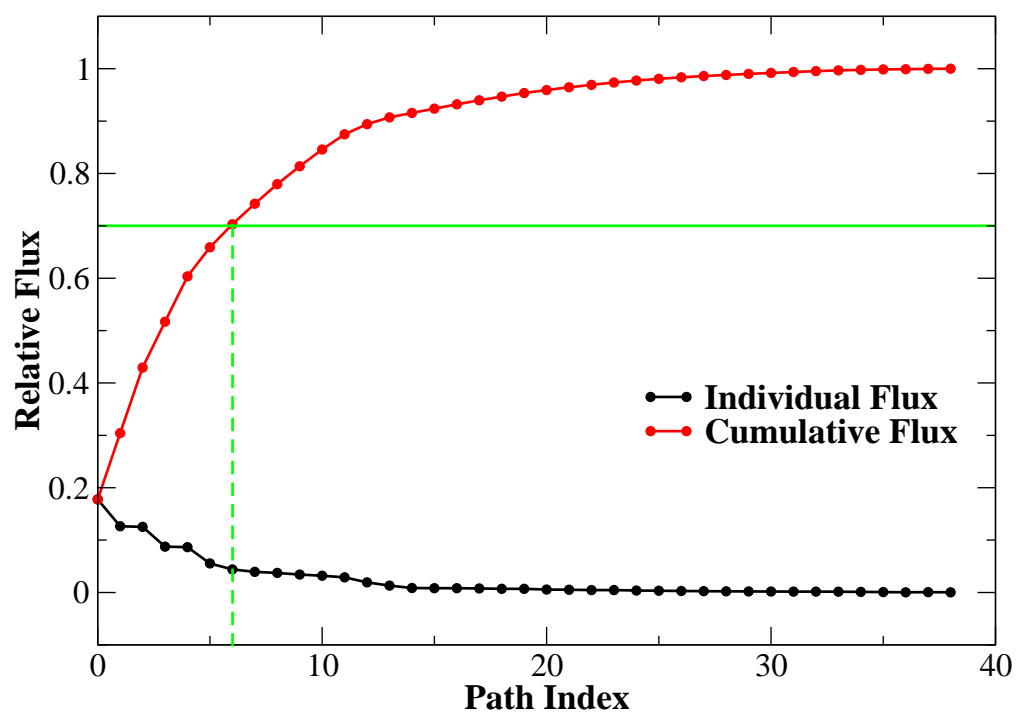


Figure 2: Fluxes of the individual permeation pathways and cumulative flux. The 7 highest-flux pathways give rise to 70% of the flux.

## NaChBac permeation

---

|                | S5-helix                      | Turret Loop | P1-helix                         |            |
|----------------|-------------------------------|-------------|----------------------------------|------------|
| <b>NaChBac</b> | IPALGNILILMSIFFYIFAVIGTMLFQHV | SPEYFGNL    | QLSLLTLFQVV                      | <b>188</b> |
| <b>NavMs</b>   | -----SVAALLTVVFYIAAVMATNLYGAT | FPEWFGDL    | SKSLYTLFQVM                      | <b>175</b> |
| <b>NavAb</b>   | ----LSVIALMTLFFYIFAIMATQLFGER | FPEWFGTL    | GESFYTLFQVM                      | <b>174</b> |
|                | SF                            | P2-helix    | S6-helix                         |            |
| <b>NaChBac</b> | TLESWAS                       | GVMRPIFAEVP | WSWLYFVSFVLLIGTFIIFNLFIGVIVNNVEK | <b>237</b> |
| <b>NavMs</b>   | TLESWSM                       | GIVRPVMNVHP | NAWVFFIPFIMLTTFTVLNLFIGII-----   | <b>224</b> |
| <b>NavAb</b>   | TLESWSM                       | GIVRPLMEVYP | YAWVFFIPFIFVVTFVMINLVVAICVDAM--  | <b>223</b> |

Figure 3: Sequence alignment of the NaChBac pore domain and the corresponding regions of NavMs and NavAb channels. The color code discriminates the sequence stretches pertaining to the different elements of the domain: S5-helix (red), Turret loop (blue), P1-helix (green), Selectivity Filter (purple), P2-helix (magenta) and S6-helix (orange).

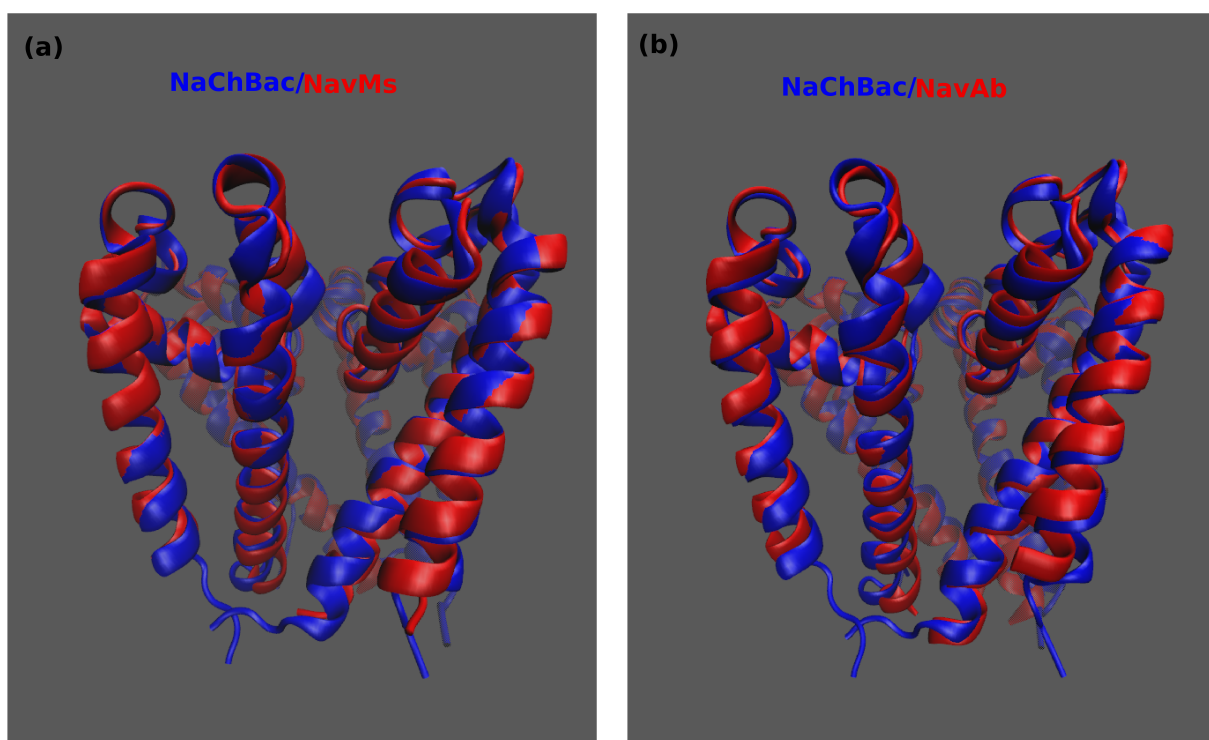


Figure 4: Superposition of the NaChBac homology model (blue) with: (a) the NavMs template (red); (b) the NavAb channel (red).

## NaChBac permeation

---

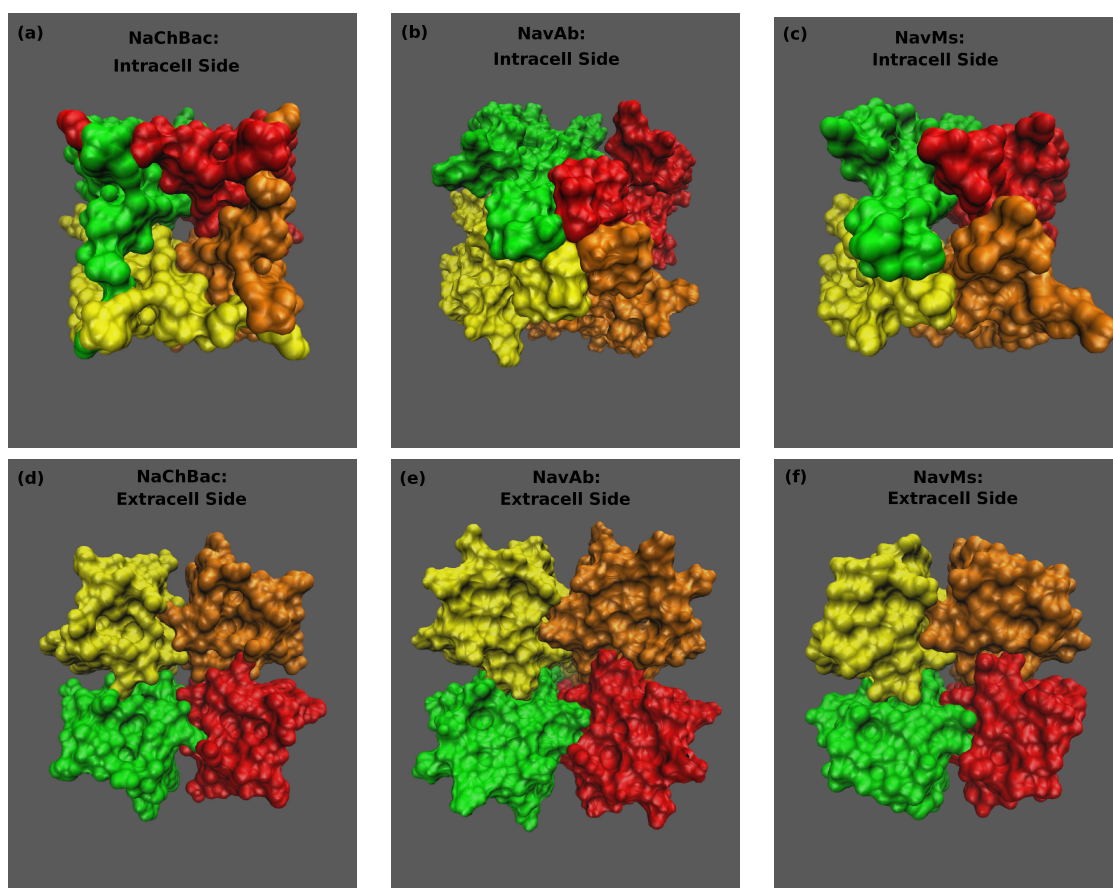


Figure 5: Space-filling representation of NaChBac (a, d), NavAb (b,e) and NavMs (c, f). A view of the channels is provided from both the intracellular side (a, b, c) and the extracellular side (d, e, f). The view from the intracellular side allows inspection of the activation gate while the view from the extracellular side shows the mouth of the Selectivity Filter.

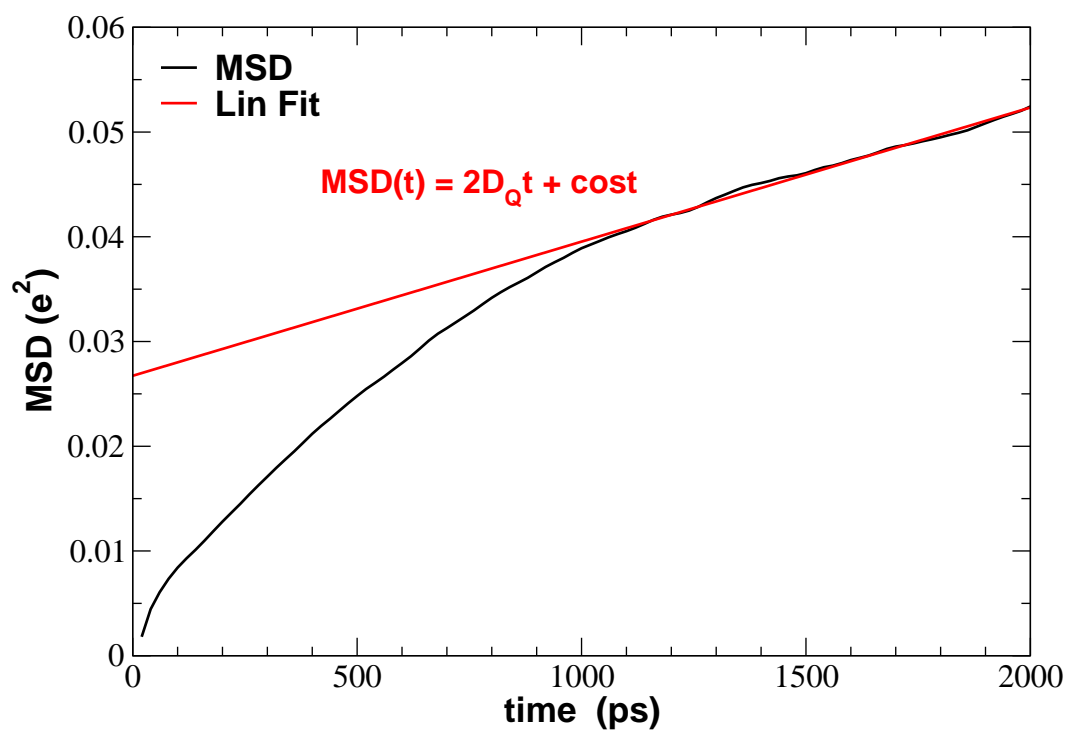


Figure 6: Computation of diffusion coefficient  $D_Q$  of the net charge transported across the channel at equilibrium, in the absence of any external electric field. Based on diffusion theory  $D_Q$  is related to the slope of the linear region of the Mean Square Displacement (MSD)  $\langle Q^2(t) \rangle$ .

## NaChBac permeation

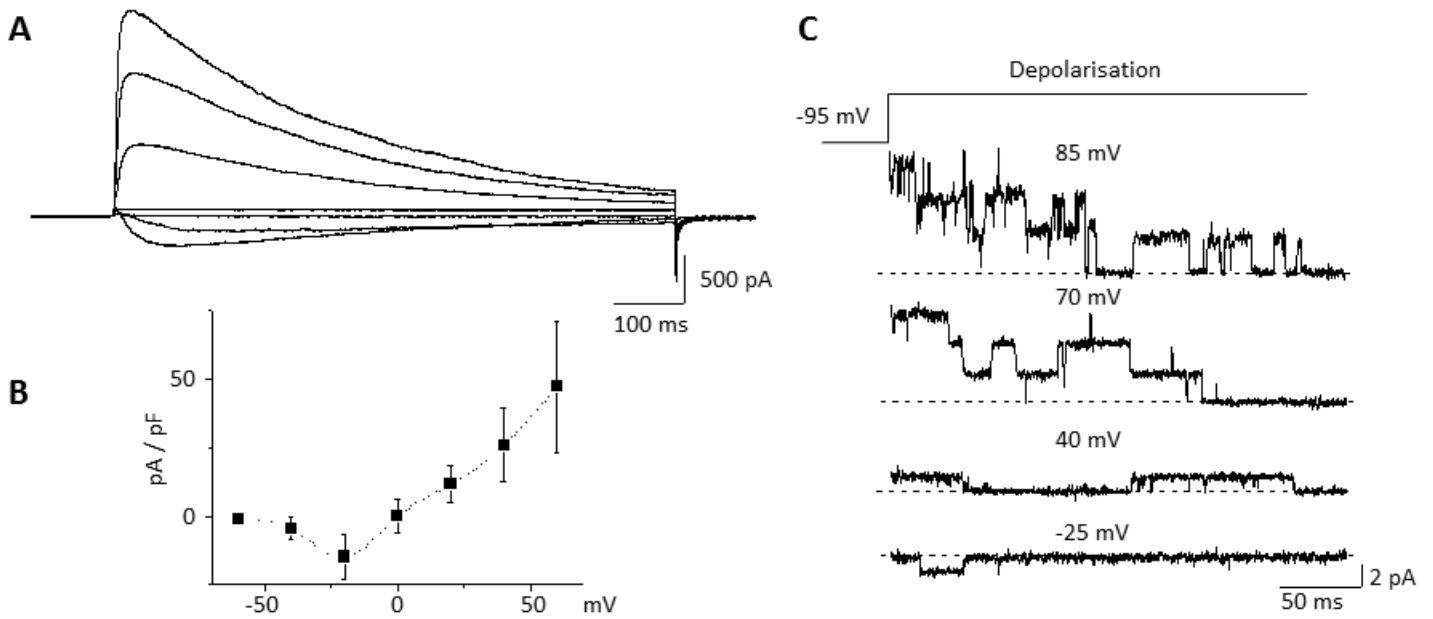


Figure 7: Patch-clamp recordings of NaChBac in 0.5 M Na<sup>+</sup>. (A) Typical whole cell currents recorded from CHO cells expressing NaChBac channels in 0.5 M Na<sup>+</sup> bath solution. (B) Whole cell peak NaChBac-mediated current-voltage relationship recorded in 0.5 M Na<sup>+</sup> bath solution. (C) Example of a single NaChBac channel activity. Recordings were made in 0.5 M Na<sup>+</sup> bath solution from an excised outside out patch. Closed state is denoted by dashed line and upward (downward for -25 mV) deflections represent the channel openings.

## NaChBac permeation

---

|            | stage-1 | stage-2 | stage-3 | stage-4 | stage-5 | stage-6 |
|------------|---------|---------|---------|---------|---------|---------|
| BB         | 10.0    | 5.0     | 2.5     | 1.0     | 0.5     | 0.1     |
| SC         | 5.0     | 2.5     | 1.0     | 0.5     | 0.1     | 0.0     |
| Lip-Head   | 5.0     | 5.0     | 2.0     | 1.0     | 0.2     | 0.0     |
| Dihed      | 500.0   | 200.0   | 100.0   | 100.0   | 50.0    | 0.0     |
| $\delta t$ | 1.0     | 1.0     | 1.0     | 2.0     | 2.0     | 2.0     |
| $T_{sim}$  | 25.0    | 25.0    | 25.0    | 200.0   | 200.0   | 200.0   |

Table 1: Parameters of NaChbac equilibration. For each stage the force constants are listed of the harmonic restrants on backbone (BB), side-chains (SC), phospholipid heads (Lip-Head), and dihedral angles (Dihed). Force constants are expressed in kcal/mol/Å<sup>2</sup>. Also shown is the time-step  $\delta t$  (in *fs*) and the duration  $T_{sim}$  (in *ps*) of each stage.